Orbital density wave induced by electron-lattice coupling in orthorhombic iron pnictides

Da-Yong Liu[1], Ya-Min Quan[1], Dong-Meng Chen[2], Liang-Jian Zou[1,*], and Hai-Qing Lin[3]

[1] *Key Laboratory of Materials Physics,*

Institute of Solid State Physics,

Chinese Academy of Sciences,

P. O. Box 1129, Hefei 230031,

People's Republic of China

[2] *College of Physics Science and Technology,*

China University of Petroleum,

DongYing 257061,

People's Republic of China

[3] *Department of Physics,*

Chinese University of Hong Kong,

Shatin, New Territory, Hong Kong, China

(Dated: Sep 20, 2010)

Abstract

In this paper we explore the magnetic and orbital properties closely related to a tetragonal-orthorhombic structural phase transition in iron pnictides based on both two- and five-orbital Hubbard models. The electron-lattice coupling, which interplays with electronic interaction, is self-consistently treated. Our results reveal that the orbital polarization stabilizes the spin density wave (SDW) order in both tetragonal and orthorhombic phases. However, the ferro-orbital density wave (F-ODW) only occurs in the orthorhombic phase rather than in the tetragonal one. Magnetic moments of Fe are small in the intermediate Coulomb interaction region for the striped antiferromangnetic phase in the realistic five orbital model. The anisotropic Fermi surface in the SDW/ODW orthorhombic phase is well in agreement with the recent angle-resolved photoemission spectroscopy experiments. These results suggest a scenario that the magnetic phase transition is driven by the ODW order mainly arising from the electron-lattice coupling.

PACS numbers: 75.30.Fv,74.20.-z,71.10.-w

I. INTRODUCTION

The recent discovery of superconductivity in $RFeAs_{1-x}O_x$ (R=La, Ce, Sm, Pr, Nd, etc.) with high transition temperature has attracted extensive interest [1]. The parent compound LaFeAsO shows strong anomalies near 150 K in resistivity, magnetic susceptibility, specific heat, *etc.*. It is suggested that the ground state is a spin-density-wave (SDW) ordered state with a striped antiferromagnetic (S-AFM) configuration [2]. The predicted magnetic structure was then confirmed by a subsequent neutron diffraction experiment [3]. Interestingly, the neutron diffraction data indicated that a subtle structural distortion occurs first at $T_s \sim 155$ K, and the SDW long-range order establishes at a slightly lower temperature, $T_{SDW} \sim 137$ K [3]. This phenomenon also has been generically found in other 1111 systems of the iron pnictides, *e.g.*, NdFeAsO (T_s and $T_{SDW} \sim 150$ K and 141K, respectively.) [4, 5], and in the 111 systems, *e.g.* NaFeAs with 52 K and 41 K [6], and in the 11 systems, *e.g.* FeTe with 87 K and 75 K [7]. However in 122 systems, the structural and magnetic phase transitions spontaneously happen, *i.e.*, at 142 K for $BaFe_2As_2$ [8], and at 205 K for $SrFe_2As_2$ [9–11], *etc.*. Although the structural phase transition occurs before the magnetic ordering is formed, it is difficult to distinguish either the instability of the electronic structure or the orthorhombic lattice distortion plays an essential role. Especially, unless there exists strong magneto-elastic coupling, it is very strange that the structural transition and the magnetic transition are so closely related.

The SDW order is suppressed by electron or hole doping, and the superconductivity is triggered in doped iron pnictides [2]. The closeness of the superconducting phase to the SDW instability implies that the AFM fluctuations play a key role in the superconducting pairing mechanism. Therefore, investigating the origin of the SDW instability in the parent compound is an essential step to understand the microcosmic origin of the superconductivity. Up to date, two main mechanisms were proposed for addressing the SAFM ordering in iron pnictides. The first one suggested that the SAFM results from the Fermi-surface nesting of itinerant electrons [2, 12–15], which is itinerant SDW character with modulation wavevector Q=(π,0). Alternatively, it was proposed that the superexchange interaction mediated through the off-plane As atom dominates the spin configuration formation [16–21]. In such a local picture, the SAFM ordering arises from the competition between the nearest-neighbor (NN) and next nearest-neighbor (NNN) spin couplings, when the NNN exchange coupling becomes larger than half of the NN exchange interaction. Whether an itinerant picture [22–24] or a localized superexchange mechanism [16, 17, 19, 20] responsible for

the SDW ordering is still a hot debate for Fe-based layered systems [25].

On the other hand, it is now believed that iron pnictides are the multi-orbital systems, with Fe^{2+} ion in a tetrahedral crystal field (CF). The energy level splittings of the five 3d orbitals are small, in a magnitude order of 0.1 eV [13, 17]. Thus the splitting is sensitive to the lattice distortion. It is found that in the high-temperature tetragonal phase, the xz and yz orbitals are degenerate [26]. While we expect such a degeneracy is removed in the low-temperature orthorhombic phase. Up to date, the minimal two-orbital model with half-filling [24, 27, 28], three-orbital model with a filling of one third (i.e., two electrons in three orbitals) [29] and a filling of two thirds (i.e., four electrons in three orbitals) [30–33], four-orbital model with half-filling [28], and full five-orbital model (with six electrons in five orbitals) in the two dimensional (2D) case [15, 32–38] and three dimensional (3D) one [39, 40], were proposed for addressing the low-T electronic, magnetic and optical properties of the iron pnictides. However, in most of previous works [27, 28, 30–34, 36], the orthorhombic CF splitting was neglected. Only a few authors suggested the role of the orthorhombic CF splitting [41–43], but the magnitude of the CF splitting was not self-consistently determined. Therefore, whether the degeneracy of the orbitals and the orthorhombic distortion play an essential role on the groundstate properties or not is still not very clear.

The remove of the degeneracy of the xz/yz orbitals may be associated with the orbital ordering (OO) in iron pnictides. In a recent angle-resolved photoemission spectroscopy (ARPES) experiment on $BaFe_2As_2$, it was found that magnetostructural transition is accompanied with orbital-dependent modifications in the electronic structure [44], which is an evidence of the orbital polarization or OO. Especially, the infrared phonon anomaly in $BaFe_2As_2$ was also thought to be the consequence of the ordering of the orbital occupation [45]. In addition, the magnetic [46], resistance [47–49] and optical conductivity [50] anisotropies were observed in the experiments, which were attributed to be the evidence of the orbital polarization. Meanwhile, the possible influence of the orbital polarization has also been investigated by many other experimental and theoretical works, including local-density approximation (LDA) [33, 34, 51]. The OO concept based on the strong correlation and localized picture, which is usually applied for classical insulator materials, had been proposed to being responsible for the SDW order [52]. However, the iron pnictides, being a bad metal and in the moderate correlation regime [53], it doesn't seem to fall into this class material. Therefore, the orbital density wave (ODW) based on itinerant scenario can be applied on these moderate correlation systems [54–57].

Although some theoretical works proposed the OO scenario [34, 51], to interpret the origin of

the orbital polarization of iron pnictides observed in experiment, other authors suggested that these results are mainly driven by the magnetic ordering in absence of the OO [33]. Recently, the strong electron-lattice (e-l) interaction associated with the orthorhombic distortion in $BaFe_2As_2$ has been suggested to take responsiblility for the structural phase transition [58], which contradicts with the scenario that the OO induced by purely electron-electron (e-e) interaction drives the structural phase transition [51]. Therefore, the origin of the orbital polarization and its consequence are still an open and debating question. As an alternative, we suggest recently that the ODW favors the existence of the SDW in iron pnictides [57]. In this paper, we propose that the SDW ordering is driven by the density wave-type OO state in iron pnictides. We find that such an OO phase is stabilized only in the presence of the orthorhombic distortion. The OO physics in five orbital model is similar to the degenerate two-orbital picture due to the Jahn-Teller-type distortion in the itinerant background. This paper is organized as follows: a model Hamiltonian and mean-field approximation are described in *Sec. II*; then the numerical results and discussions are presented in *Sec. III*; the last section is devoted to the remarks and summary.

II. EFFECTIVE HAMILTONIAN AND ORDERING PARAMETERS

We start with an extend multi-orbital Hubbard model Hamiltonian including both the e-e and e-l interactions,

$$H = H_0 + H_I + H_{e-l}. \tag{1}$$

Here H_0 describes the kinetic energy term,

$$H_0 = \sum_{\substack{i,j \\ \alpha,\beta,\sigma}} t_{ij}^{\alpha\beta} C_{i\alpha\sigma}^{+} C_{j\beta\sigma} - \mu \sum_{i\alpha\sigma} n_{i\alpha\sigma} \tag{2}$$

where $C_{i\alpha\sigma}^{+}$ creates an electron on site i with orbital α and spin σ, $t_{ij}^{\alpha\beta}$ is the hopping integral between the i site with α orbital and the j site with β orbital, and μ is the chemical potential determined by the electron filling. The electronic interaction part reads,

$$\begin{aligned} H_I = & U \sum_{i,\alpha} n_{i\alpha\uparrow} n_{i\alpha\downarrow} + U' \sum_{\substack{i \\ \alpha\neq\beta}} n_{i\alpha\uparrow} n_{i\beta\downarrow} + (U' - J_H) \sum_{i,\sigma} n_{i1\sigma} n_{i2\sigma} \\ & - J_H \sum_i (C_{i1\uparrow}^{+} C_{i1\downarrow} C_{i2\downarrow}^{+} C_{i2\uparrow} + h.c.) + J_H \sum_i (C_{i1\uparrow}^{+} C_{i1\downarrow}^{+} C_{i2\downarrow} C_{i2\uparrow} + h.c.) \end{aligned} \tag{3}$$

where U(U$'$) denotes the intra-(inter-)orbital Coulomb repulsion interaction and J_H the Hund's coupling. We take U$'$=U-2J_H throughout this paper.

The e-l interaction is depicted as

$$H_{e-l} = \frac{\delta}{2}\sum_{i\sigma}(n_{i1\sigma} - n_{i2\sigma})e^{i\vec{Q}_o\cdot\vec{R}_i} + \frac{\lambda}{2}\sum_i \delta_i^2 \tag{4}$$

where δ is the CF level splitting of the xz and yz orbitals induced by orthorhombic distortion, and $\vec{Q}_o$ is the ODW vector, λ is a constant coefficient. Since the metallic iron pnictides do not fall into conventional OO scenario for insulators, it is only a SDW-type spin ordering and ODW-type OO for complicated metals [57]. In the presence of the SDW and ODW order, we adopt the following mean-field approximation in real space to decouple the particle-particle interaction terms in Eq. (3),

$$< n_{i\alpha\sigma} > = \frac{1}{4}[n_{12} + \sigma m_s e^{i\vec{Q}_s\cdot\vec{R}_i} + \alpha m_o e^{i\vec{Q}_o\cdot\vec{R}_i} + \sigma\alpha m_{so} e^{i(\vec{Q}_s+\vec{Q}_o)\cdot\vec{R}_i}]. \tag{5}$$

For the α orbitals (1=zx and 2=yz) in iron pnictides, and for the electrons in β orbitals with $\beta = 3 : x^2 - y^2, 4 : xy, 5 : 3z^2 - r^2$, we adopt,

$$< n_{i\beta\sigma} > = \frac{1}{2}[n_\beta + \sigma m_\beta e^{i\vec{Q}_s\cdot\vec{R}_i}] \tag{6}$$

where we define the particle numbers $n_{12} = \frac{1}{N}\sum_{k\sigma,\alpha=1,2} < C^+_{k\alpha\sigma}C_{k\alpha\sigma} >$, $n_\beta = \frac{1}{N}\sum_{k\sigma} < C^+_{k\beta\sigma}C_{k\beta\sigma} >$, and the SDW/ODW order parameters $m_s = \frac{1}{N}\sum_{k\sigma,\alpha=1,2}\sigma < C^+_{k\alpha\sigma}C_{k-Q_s\alpha\sigma} >$, $m_o = \frac{1}{N}\sum_{k\sigma,\alpha=1,2}\alpha < C^+_{k\alpha\sigma}C_{k-Q_o\alpha\sigma} >$, $m_{so} = \frac{1}{N}\sum_{k\sigma,\alpha=1,2}\sigma\alpha < C^+_{k\alpha\sigma}C_{k-Q_s-Q_o\alpha\sigma} >$, $m_\beta = \frac{1}{N}\sum_{k\sigma}\sigma < C^+_{k\beta\sigma}C_{k-Q_s\beta\sigma} >$, respectively. In the momentum space the decoupled effective Hamiltonian can be written as

$$H_0 = \sum_{k,\alpha,\beta,\sigma}[T^{\alpha\beta}(\vec{k})C^+_{k\alpha\sigma}C_{k\beta\sigma} + T^{\beta\alpha}(\vec{k})C^+_{k\beta\sigma}C_{k\alpha\sigma} - \mu C^+_{k\alpha\sigma}C_{k\alpha\sigma}] \tag{7}$$

and

$$\begin{aligned}\tilde{H}_I = & \sum_{\substack{k,\sigma\\ \alpha=zx,yz}}[(AC^+_{k\alpha\sigma}C_{k\alpha\sigma} + \sigma BC^+_{k,\alpha\sigma}C_{k-Q_s\alpha\sigma} \\ & +\alpha CC^+_{k\alpha\sigma}C_{k-Q_o\alpha\sigma} + \sigma\alpha DC^+_{k\alpha\sigma}C_{k-Q_s-Q_o\alpha\sigma})] \\ & + \sum_{\substack{k\sigma\\ \beta=x^2-y^2,xy,3z^2-r^2}}[(E_\beta C^+_{k\beta\sigma}C_{k\beta\sigma} + \sigma F_\beta C^+_{k\beta\sigma}C_{k-Q_s\beta\sigma})] + const.\end{aligned} \tag{8}$$

where the coefficient $A = \frac{1}{4}n_{12}U + \frac{1}{2}(\frac{1}{2}n_{12} + n_3 + n_4 + n_5)(2U' - J_H)$, $B = -\frac{1}{4}m_sU - \frac{1}{2}(\frac{1}{2}m_s + m_3 + m_4 + m_5)J_H$, $C = \frac{1}{4}m_o[U - 2U' + J_H]$,$D = -\frac{1}{4}m_{so}[U - J_H]$, $E_\beta = \frac{1}{2}n_\beta U + \frac{1}{2}(n_{12} + n_{\bar{\beta}})(2U' - J_H)$,

and $F_\beta = -\frac{1}{2}m_\beta U - \frac{1}{2}(m_s + m_{\bar{\beta}})J_H$. The constant term reads

$$\begin{aligned} const. \;=\; & -\frac{N}{4}U[\frac{1}{2}(n_{12}^2 + m_o^2 - m_s^2 - m_{so}^2) + n_3^2 + n_4^2 + n_5^2 - m_3^2 - m_4^2 - m_5^2] \\ & -NU^{'}[\frac{1}{4}(n_{12}^2 - m_o^2) + n_{12}(n_3 + n_4 + n_5) + n_3n_4 + n_3n_5 + n_4n_5] \\ & +\frac{N}{2}J_H[\frac{1}{4}(n_{12}^2 + m_s^2 - m_o^2 - m_{so}^2) + n_{12}(n_3 + n_4 + n_5) + n_3n_4 + n_3n_5 + n_4n_5 \\ & +m_s(m_3 + m_4 + m_5) + m_3m_4 + m_3m_5 + m_4m_5] \end{aligned} \tag{9}$$

The e-l interaction describing the orthorhombic distortion is expressed as

$$H_{e-l} = \frac{\delta}{2}\sum_{k,\sigma}(C_{kzx\sigma}^{+}C_{k-Q_ozx\sigma} - C_{kyz\sigma}^{+}C_{k-Q_oyz\sigma}) + \frac{N\lambda}{2}\delta^2 \tag{10}$$

Minimizing the groundstate energy with respect to the energy level splitting gives rise to the level splitting $\delta = -\frac{1}{2N\lambda}\sum_{k\alpha\sigma}\alpha < C_{k\alpha\sigma}^{+}C_{k-Q_o\alpha\sigma} >$. Thus the CF splitting δ can be obtained self-consistently by $\delta = -\frac{1}{2}m_o/\lambda$.

III. RESULTS AND DISCUSSIONS

In this section, we first present our studies for the two orbital model, and then for the more realistic five orbital model of the quasi-two-dimensional systems, such as 1111 phase (LaOFeAs, etc.), within the mean-field approximation, finally extend to the three-dimensional systems in the 122 phase ($BaFe_2As_2$, etc.). The magnetic and orbital properties closely related with a tetragonal-orthorhombic structural phase transition in the iron pnictides are explored. In addition, the effect of the inter-player coupling for $BaFe_2As_2$ is also considered in the five orbital model.

A. Two-Orbital Model

We firstly present our results in the case of the two-orbital model [24]. The possible spin and orbital configurations with modulation wave-vectors Q_s/Q_o=(0,0),(0,π),(π,0) and (π,π) in both the tetragonal structure and the orthorhombic phase are studied. Note that in the tetragonal phase, the orthorhombic distortion is absent, i.e. $H = H_0 + \tilde{H}_I$; for comparison, while in the orthorhombic phase the orthorhombic distortion is present, i.e. $H = H_0 + \tilde{H}_I + H_{e-l}$. The J_H-U phase diagrams are obtained both for the tetragonal phase and for the orthorhombic one, as shown in Fig. 1 (a) and (b). In the tetragonal case, the SAFM metallic phase is a stable ground state with small magnetic

moment in the intermediate Coulomb interaction parameter region, and all the orbital configurations are degenerate in the SAFM phase, as seen in Fig. 1 (a). So the ground state is nearly a para-orbital or orbital liquid phase. However in the orthorhombic phase, the e-l coupling breaks the orbital degeneracy of the xz-orbit and the yz-orbit, leading to a ferro-orbital (FO) configuration. Due to the itinerant character of the electron, the orbital polarization in the ODW state is small. Since the pure electronic interaction is insufficient to contribute the FO-SAFM phase, the Jahn-Teller-type orthorhombic distortion removing the xz- and yz-orbital degeneracy results in a weak FO ordering phase. While, in the large U parameter region, the OO is destroyed under the strong Coulomb interaction, which favors electron occupation in the xz and yz orbitals equally. In addition, the FO phase absence of SDW appears in the weak Hund's coupling region, which is the result of the competition between the crystal field splitting and the Hund's copling. Here, the elastic coefficient parameter λ is fixed to be 0.5/t (t is the hopping integral parameter in Ref. [24]) for the two-orbital model throughout this paper.

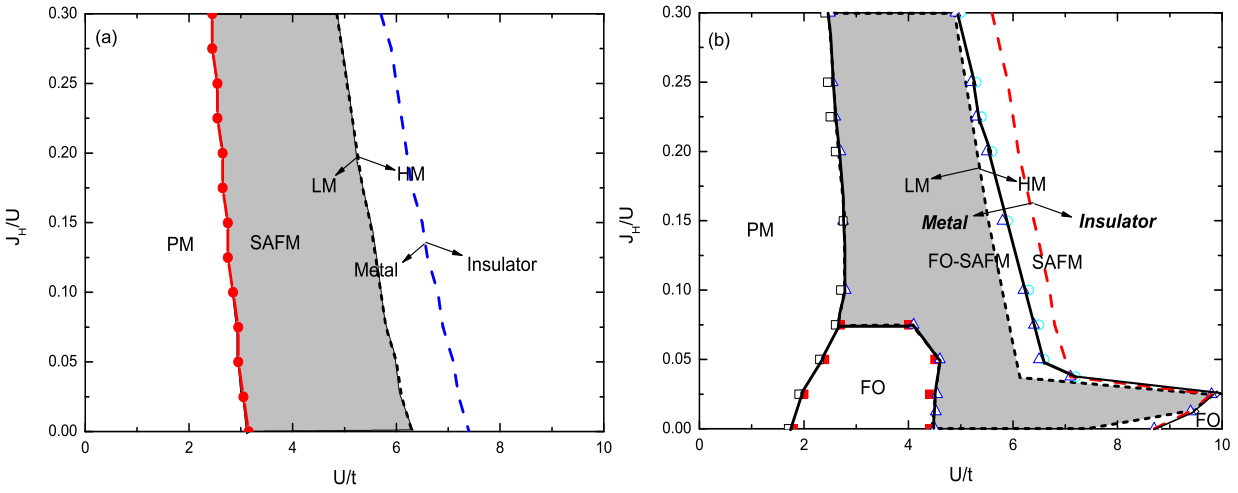

FIG. 1: J_H-U phase diagram of the two-orbital model in the tetragonal (a) and orthorhombic (b) phases. PM and SAFM denotes paramagnetic and striped antiferromagnetic (Q_s=$(\pi, 0)$) phase, respectively. FO represents the ferro-orbital order with Q_o=$(0, 0)$. The solid lines with different symbols display different phase boundaries. The dash line and short dash line denote the the metal-insulator border and the low magnetic (LM) moment($\mu < 1\ \mu_B$) and high magnetic (HM) moment ($\mu > 1\ \mu_B$) phase border, respectively.

Minimizing the groundstate energy, we self-consistently obtain the orthorhombic CF splitting, $\delta = -\frac{1}{2}m_o/\lambda$, for the orthorhombic case. In Fig. 2, the dependence of the CF splitting between the xz- and yz-orbit on the elastic coefficient λ is plotted with the Coulomb repulsion U=4t for

different Hund's coupling J_H. For small coefficient λ, the CF splitting δ becomes larger under the strong e-l interaction. However, the large Hund's coupling obviously suppresses the CF splitting, since the Hund's coupling tends to distribute the electrons in two orbitals equal-weightly. This is also seen in Fig.1(b), the FO phase only exists for small J_H.

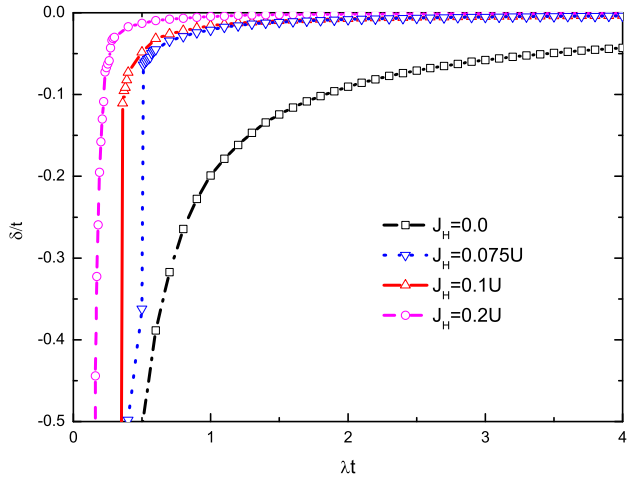

FIG. 2: Dependence of the crystal field splitting δ in the orthorhombic case on the elastic coefficient λ in two-orbital model, with the parameters U=4t for J_H=0, 0.075U ,0.1U and 0.2U.

It is known that the SDW, ODW and combined spin-orbital density wave order parameters, m_s, m_o and m_{so}, crucially depends on the Coulomb interaction. The comparison between the tetragonal and the orthorhombic phases are displayed in Fig. 3. Although the ordering parameters are rather small, an obvious orbital polarization occurs in the orthorhombic case in the intermediate Coulomb interaction range. As a comparison, it is absent in the tetragonal case. A rather small SAFM magnetic moment is also obtained in the intermediate coupling region, as seen in the shadow region of Fig. 3. Notice that with the increase of U, the crossover of the orbital polarizations from the xz-type symmetry to the yz-type one occurs at $U_c \sim 4.5t$.

To compare partial density of state (PDOS) in both tetragonal and orthorhombic cases are plotted in Fig. 4. It is shown that there is no orbital polarization in the non-interacting case at U=0. With the increase of U to a region of $U_1 \sim 2.8t < U < U_c$, the PDOS of the xz-orbital component is larger than that of the yz-orbital component near Fermi surface in orthorhombic case, indicating an obvious xz-orbital polarization. However, further increasing U to the region of $U_c < U < U_2 \sim 5.8t$, it changes to a weak yz-orbital polarization, in agreement with Fig. 3. In the orthorhombic phase, there exists larger orbital polarization than that in the tetragonal phase. Obviously, although the electronic interaction plays a key role in the orbital polarization, the e-l interaction finally stabilizes

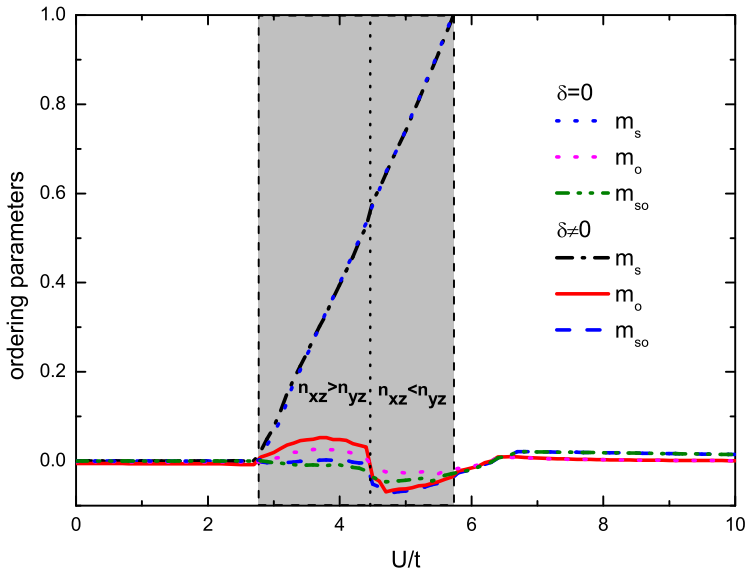

FIG. 3: Dependence of the spin, orbital and spin-orbital ordering parameters on Coulomb interaction in the tetragonal (δ=0) and orthorhombic ($\delta\neq0$) phases, with J_H=0.1U. The vertical dashed dotted line denotes the boundary of different orbital polarization. The shadow region represents the small magnetic moment case ($< 1\,\mu_B$).

the ground state of the LaOFeAs to the FO-type SAFM phase.

To get a further insight into the SDW and ODW states, we display the evolution of the Fermi surface on the Coulomb interaction in the folded Brillouin zone of SAFM phase in Fig. 5. The Fermi surface nesting is obviously observed in the non-interacting paramagnetic case, including two hole pockets at the center and two electron pockets at the corners of the Brillouin zone. Nevertheless, with the increasing of the electronic interaction, the nesting becomes weak and the ordered SAFM state is stabilized.

In addition, both the hole doping and the electron doping behaviors are investigated in this two-orbital model, the results similar to Ref.[27] are obtained. Comparing with the experiments, we find that in the hole doped case, the magnetic moment decreases with doping, and is concordant with the experimental results [2]. While the AFM moment increases with the increase of electron doping, which is completely in contradiction to the experimental observations [2]. On the other hand, the Fermi surface of the ordered state and the xz-orbital polarization character of the Fermi surface in the two-orbital model are not in agreement with the recent ARPES experiments [44]. To resolve these discrepancies, we have to extend the present effective two-orbital model to the realistic five-orbital model.

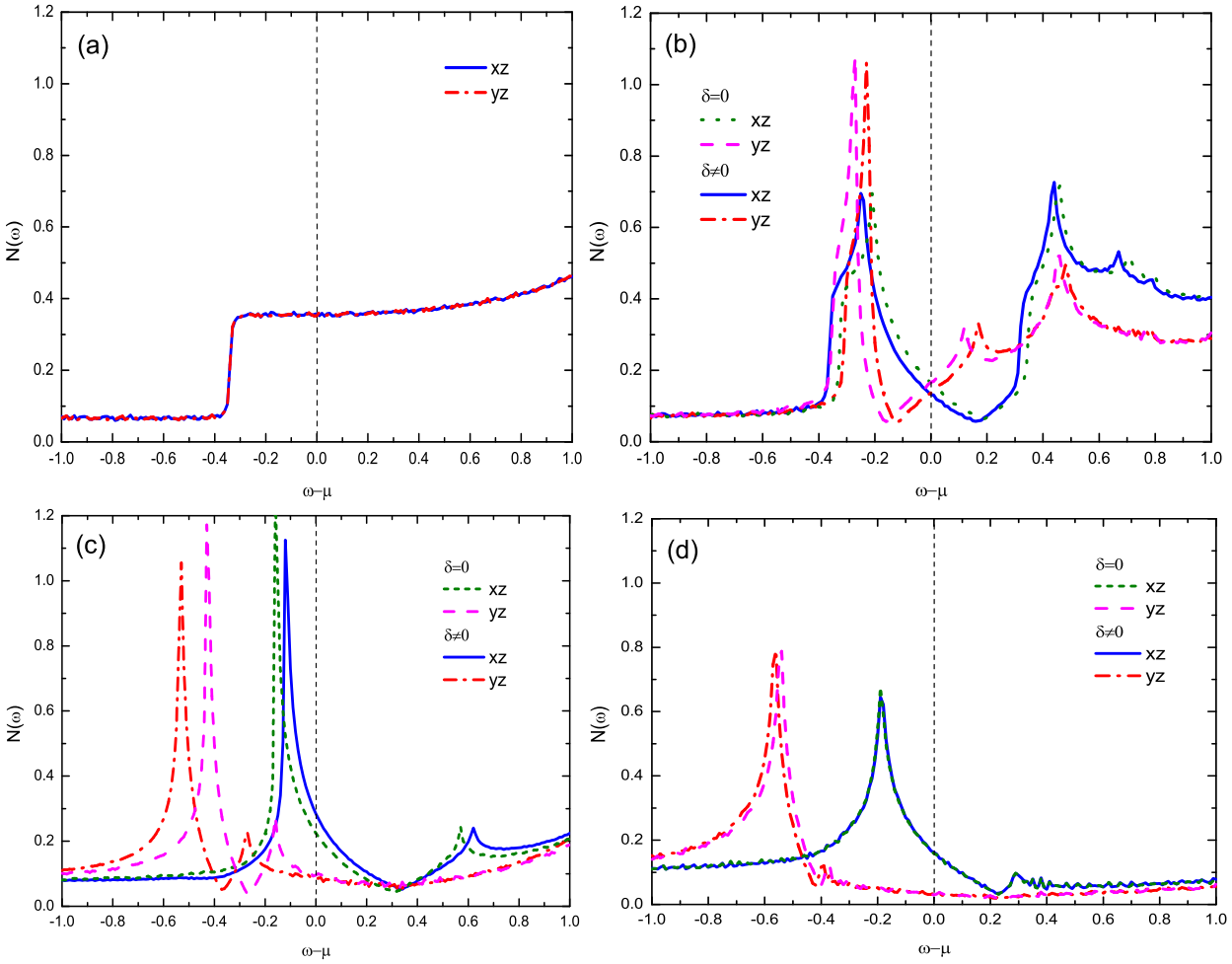

FIG. 4: Partial density of states in the tetragonal (δ=0) and orthorhombic ($\delta\neq0$) structures for different Coulomb parameters U=0 (a), 4t (b), 5t (c), and 6t (d) with J_H=0.1U.

B. Five Orbital Model

It is now generally believed that the more orbitals other than two orbitals are involved in the low-energy physics in iron pnictides. The five orbital of 3d electrons of Fe^{2+} in the tetrahedral CF should be considered to address the electronic, magnetic and orbital properties of the iron pnictides. In this subsection, we explore the role of the e-l coupling within the five-orbital model [35]. Notice that, unless otherwise specified, the elastic coefficient parameter λ is fixed to be 1.0 eV^{-1} for the five-orbital model throughout this paper. Phase diagram of the five-orbital model for the tetragonal (a), and orthorhombic (b) phases are shown in Fig. 6. It is clearly found that the FO phase is in a stable ground state in the presence of the orthorhombic distortion. The intermediate Coulomb interaction with a weak Hund's coupling favors the SAFM phase with low magnetic

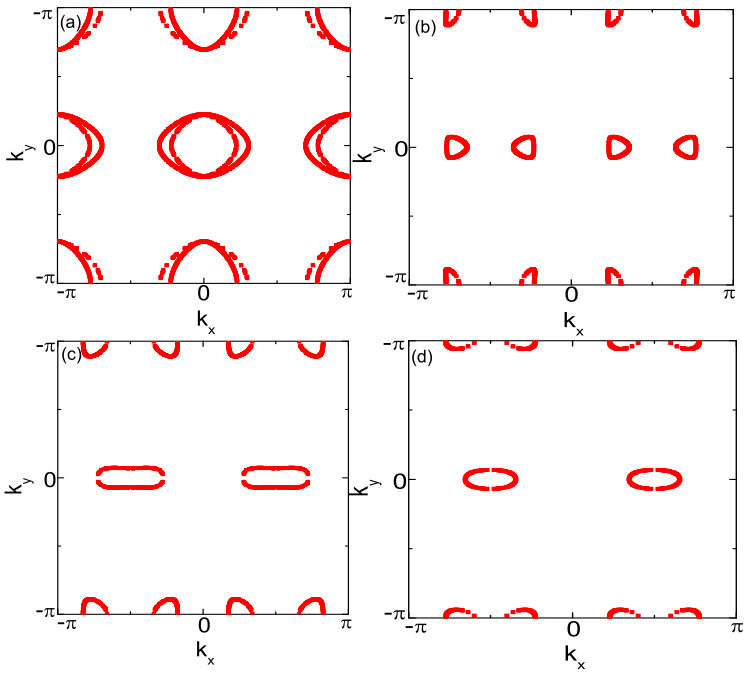

FIG. 5: Evolution of Fermi surface of the two-orbital models in the folded Brillouin zone (a) U=0, (b) 4t, (c) 5t, and (d) 6t with J_H= 0.1U for the orthorhombic phase.

moments, similar to the two-orbital model. However, the five-orbital results are obviously different from that of the two-orbital model in Fig.1(a) and Fig.1(b). With the increase of the electronic Coulomb interaction, the Néel AFM phase with Q_s=(π, π) is in the ground state. Moreover, in strong Coulomb repulsion and large Hund's coupling region, the ground state of the system is the FO-SAFM phase with large magnetic moment (μ>1 μ_B) due to the Hund's coupling. This result is obviously different from the one without FO in the simple two orbital case, which implies the five orbital case involves a complicated multi-orbital correlated effect. Further increasing the Coulomb correlation leads the system transit to insulator.

The dependence of the magnetization of each orbital, and the orbital occupancy, on the Coulomb interaction in both the tetragonal and the orthorhombic structure are obtained, the orthorhombic case is shown in Fig. 7. One finds that the xz-orbital polarization is larger than that in the tetragonal one in a very narrow intermediate Coulomb repulsion region from U=1.2 to 1.45 eV for J_H=0.25U. In this region, the low magnetization, 0<μ<1 μ_B, with bad metallic state is also obtained. The electron occupancy in the xz-orbit is always more than that in the yz-orbit as the Coulomb interaction increases. No orbital occupancy crossover from the xz-type to the yz-type symmetry is observed, which is different from the two-orbital results above. This shows that the

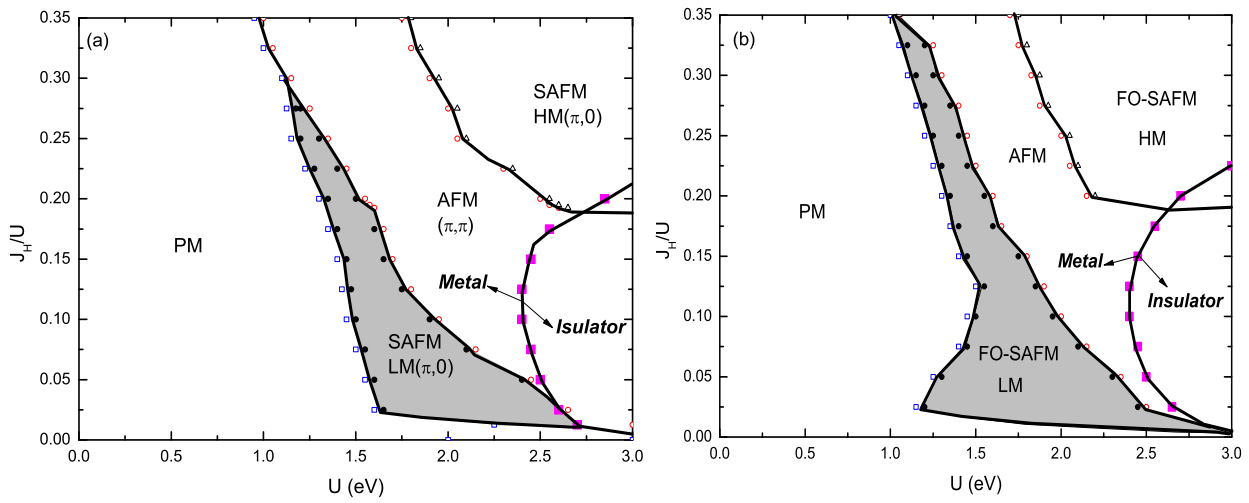

FIG. 6: J_H-U phase diagram of the five-orbital model for the tetragonal (a) and orthorhombic (b) phases, respectively. PM, SAFM and AFM denotes paramagnetic, striped antiferromagnetic (Q_s=$(\pi, 0)$) and N*é*el antiferromagnetic (Q_s=(π, π)) phases, respectively. FO represents the ferro-orbital order with Q_o=$(0, 0)$. LM and HM denote the low magnetization (μ<1 μ_B) and high magnetization (μ>1 μ_B), respectively.

ferro- xz-orbital polarization arises from the electronic interaction of the five 3d orbitals, while the long range ordering, i.e. OO is contributed from the e-l interaction. Our results are consistent with not only the crystal structure but also the ARPES experimental results [44], where the xz-orbital polarization is observed near the Γ point.

In the present five-orbital model, the orthorhombic CF splitting of the xz- and yz-orbit is also determined self-consistently. The dependence of the CF splittings on the e-l coupling, shown in Fig. 8, is similar to that in two-orbital situation. On the other hand, in contrast to the two-orbital case, where the Hund's coupling suppresses the CF splitting, the influence of the Hund's coupling on the CF splitting is complicated in the five-orbital model because of the multi-orbital effects. Either the strong or the weak Hund's coupling J_H favors the large orthorhombic CF splitting. Hence, it indicates that the orthorhombic distortion is associated with the multi-orbital effect. Thus, due to the xz-orbital polarization with the ODW of wave vector $(0, 0)$, it suffers an orthorhombic distortion, leading to that the lattice parameter *a* is larger than *b*, as experimentally observed.

In Fig. 9, the PDOS are plotted for various magnetic configurations: non-magnetic, FO-SAFM(LM), N*é*el AFM without OO, and FO-SAFM(HM), respectively. In the non-interacting (a) and FO-SAFM (b) cases, three t_{2g} orbitals, xz, yz and xy components, mainly contribute to the FS, which agrees with the LDA calculations [26] and the ARPES experiments [59]. In non-

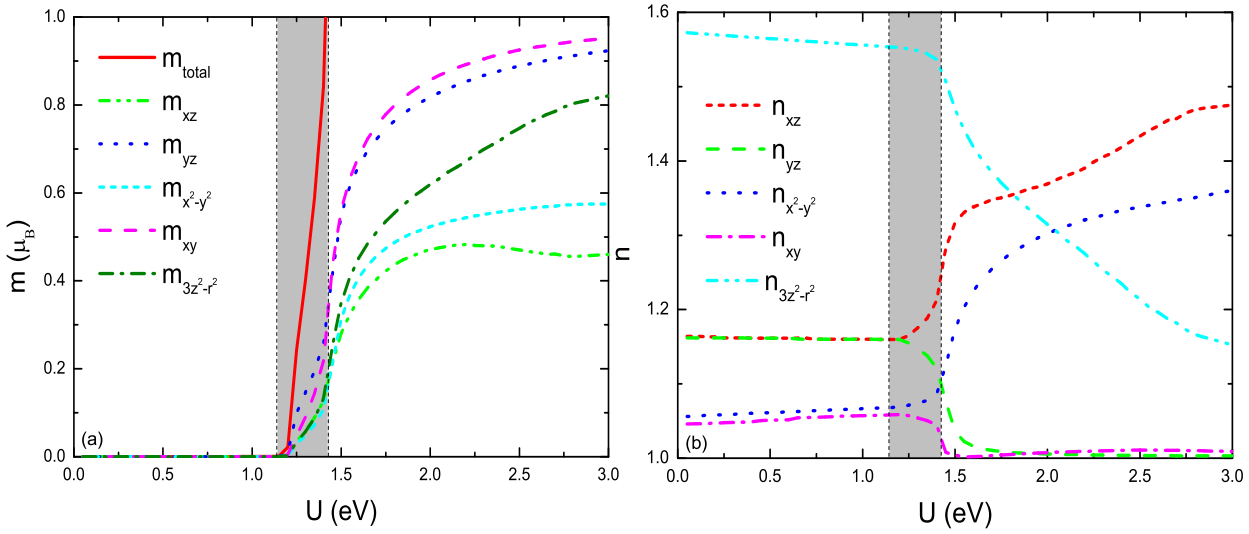

FIG. 7: Dependence of total magnetic moment, orbital magnetization (a), and orbital occupancy (b) on Coulomb interaction in the orthorhombic structure for J_H=0.25U. The shadow region denotes the small magnetic moment physical parameters region with μ<1 μ_B.

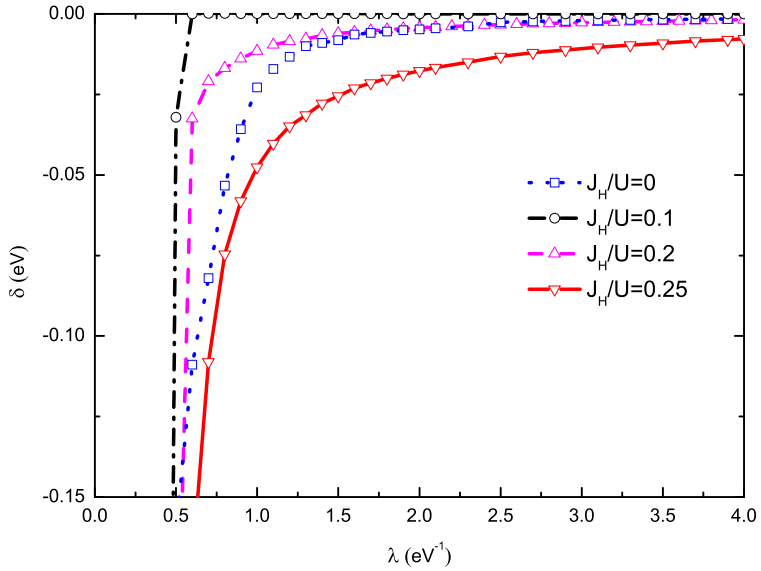

FIG. 8: Dependence of the crystal filed splitting of *xz* and *yz* orbitals on the elastic coefficient with U=1.4 eV for different Hund's rule coupling. Other parameters are the same with Fig.7

magnetic case, there is no orbital polarization of xz and yz orbitals in FS. While in the small magnetic moment phase, the PDOS of the xz-component is larger than that of the yz-component, indicating the orbital polarization is mainly xz-component, as seen in Fig. 9(b). In the Néel AFM phase with $Q_o=(\pi,\pi)$, the $3z^2-r^2$ orbital mainly contribute to the FS. On the other hand, in the FO-

SAFM(HM) phase, there is also an obvious xz-orbital polarization near the FS. Notice that due to the large magnetic moment and strong Coulomb interaction, the electrons are localized electrons rather than itinerant electrons in the SAFM states.

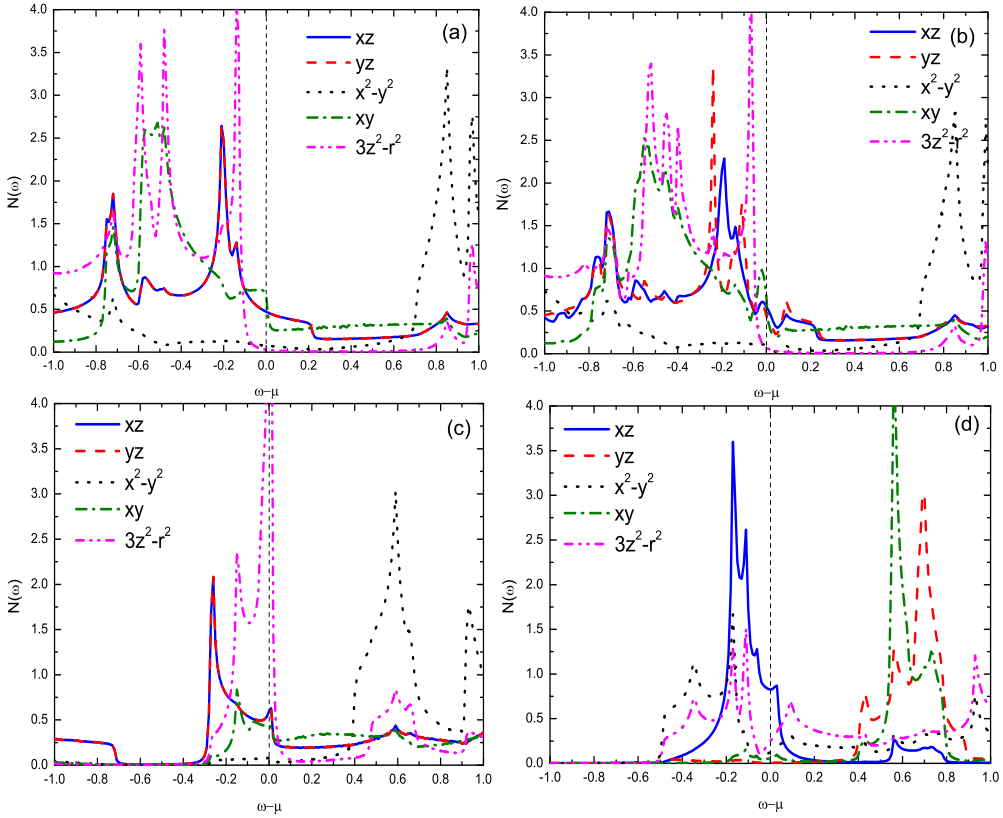

FIG. 9: Partial density of states in the paramagnetic (a), FO-SAFM(LM) (b), Néel AFM (c), and FO-SAFM (HM) (d) phases in the orthorhombic phase, with parameters U=0, 1.25, 1.75 and 2.25 eV, respectively. The Hund's coupling J_H=0.25U is adopted.

With the increase of the Coulomb interaction, the evolution of the FS is displayed in Fig. 10. From the PM state to the FO-SAFM state, the FS nestings are destroyed with the increasing electronic correlations. However, in the *Néel* AFM states, the FS nesting remains, which leads to the (π, π) AFM states. With the further increasing strong Coulomb interaction, the FS nestings become weak. Especially, the anisotropy of the FS appears in the SDW/ODW state at the Coulomb interaction U~1.25 eV, with a larger hole pockets along $\Gamma-Y(0,\pi)$ in the folded SDW/ODW Brillouin zone corresponding to the ferro-magnetic direction and a smaller one along $\Gamma-X(\pi,0)$ corresponding to the anti-ferromagnetic direction in the SAFM state. The anisotropic character of the FS resembles the results of the recent ARPES experiments [60]. The anisotropic FS is obviously

different from the FS observed in other ARPES experiments [61] and the de Haas-van Alphen experiment [62]. Furthermore, with the increase of U to 1.4 eV, the anisotropy becomes weak, with the FS along $\Gamma - Y$ direction disappearing. Our results reveal that the anisotropic character of the FS and other properties are mainly due to the splitting of xz and yz orbitals in the orthorhombic phase. Hence the anisotropy is obviously manifested by the e-l coupling.

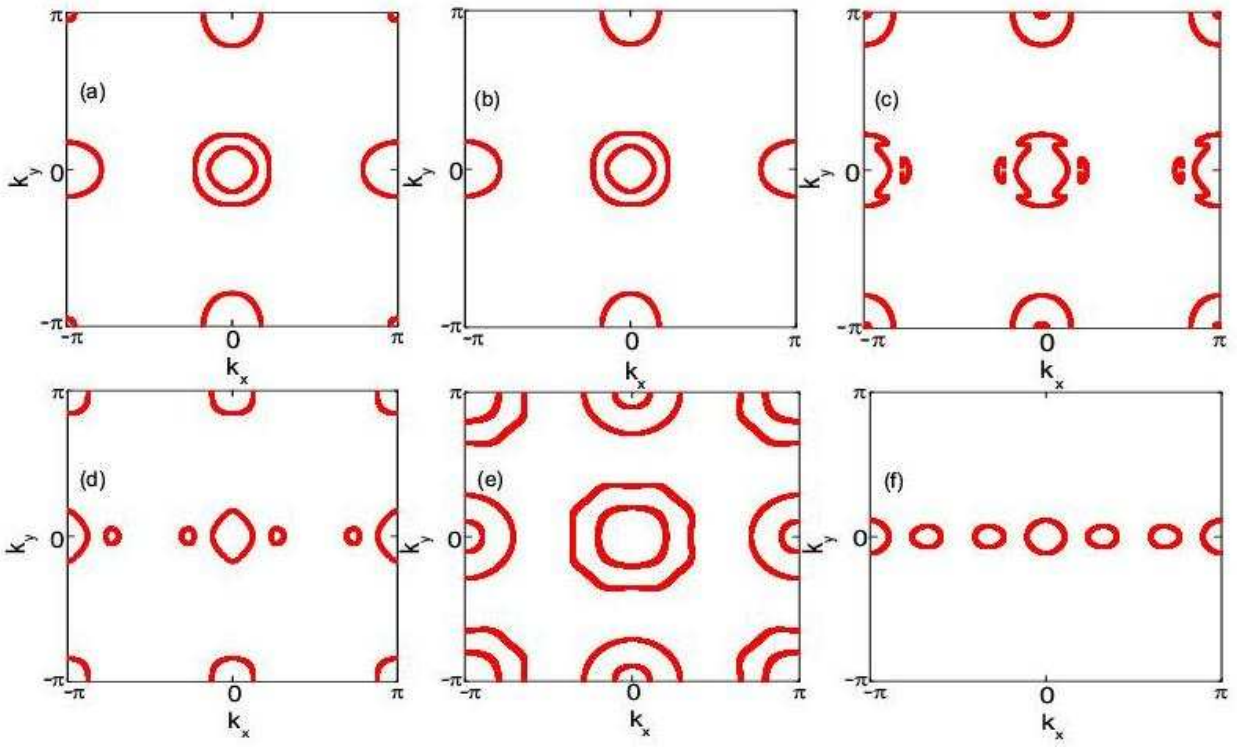

FIG. 10: Evolution of Fermi surface in the nonmagnetic/paramagnetic (a) and (b), FO-SAFM of LM (c) and (d), Néel AFM (e), and FO-SAFM of LM (f) phases in the orthorhombic phase, with the Coulomb correlation parameters are U=0 (a), 1.0 (b), 1.25 (c), 1.4 (d), 1.75 (e), and 2.25 (f) eV. J_H=0.25U is adopted.

To compare with the two-orbital model, we also investigate the doping case in the five-orbital model. We find that either hole or electron doping results in the decrease of the magnetic moment, which is well consistent with the experimental observations [2]. It is also implied that the five-orbital model is a more accurate realistic model which well describes the low-energy physics in the iron pnictides.

IV. SUMMARY

In this work, we also study the realistic five-orbital model [39] for $BaFe_2As_2$ of more 3D systems, with the SDW vector Q_s=(π,0,π), and ODW vector Q_o=(0,0,0) observed experimentally. To investigate the relationship between the structural and magnetic phase transition, the dependence of the magnetization and the ODW ordering parameters on temperature in the tetragonal and orthorhombic structures is observed. Note that the evolution of sublattice magnetization on temperature reflects the variation of the spin alignments and the long range order,. and the sublattice magnetization vanishes at the critical temperature, characterized by T_{SDW}; while the evolution of the OO parameters associated with the orthorhombic CF splitting reflects the structural phase transition, which is characterized by T_s. In absence of the orthorhombic distortion, the pure electronic interaction leads to $T_s < T_{SDW}$, contrast to the experimental results. However, in the presence of the orthorhombic distortion, $T_s \gtrsim T_{SDW}$. Therefore, in addition to the e-e interaction, addressing the e-l interaction associated with the orthorhombic distortion clearly is crucial to explain the magnetic and structural phase transitions observed experimentally. Our results support a scenario that the magnetic phase transition is driven by the ODW which is mainly induced by the orthorhombic lattice distortion in the presence of the intermediate electronic correlation.

In summary, we have presented the spin and orbital polarizations, as well as SDW and ODW ordering, in both the tetragonal and orthorhombic phase, and uncovered the relation between the structural and magnetic phase transition. We have shown that the orthorhombic lattice distortion is an essential factor to stabilize the SAFM ground state through the formation of ODW ordering.

Acknowledgments

This work was supported by the NSFC of China No. 11047154, 11074257, 10947125, and the Knowledge Innovation Program of the Chinese Academy of Sciences, and Natural Science Foundation of Anhui Province No. 11040606Q56. Numerical calculations were performed at the Center for Computational Science of CASHIPS.

[1] Y. Kamihara, T. Watanabe, M. Hirano, and H. Hosono, J. Am. Chem. Soc. **130**, 3296 (2008).

[2] J. Dong, H. J. Zhang, G. Xu, Z. Li, G. Li, W. Z. Hu, D. Wu, G. F. Chen, X. Dai, J. L. Luo, Z. Fang and N. L. Wang, Europhys. Lett. **83**, 27006 (2008).

[3] C. de la Cruz, Q. Huang, J. W. Lynn, J. Y. Li, W. Ratcliff II, J. L. Zarestky, H. A. Mook, G. F. Chen, J. L. Luo, N. L. Wang and P. C. Dai, Nature (London) **453**, 899 (2008).

[4] Y. Chen, J. W. Lynn, J. Li, G. Li, G. F. Chen, J. L. Luo, N. L. Wang, P. C. Dai, C. dela Cruz, and H. A. Mook, Phys. Rev. B **78**, 064515 (2008).

[5] Y. Qiu, W. Bao, Q. Huang, T. Yildirim, J. M. Simmons, M. A. Green, J. W. Lynn, Y. C. Gasparovic, J. Li, T. Wu, G. Wu, and X. H. Chen, Phys. Rev. Lett. **101**, 257002 (2008).

[6] G. F. Chen, W. Z. Hu, J. L. Luo, and N. L. Wang, Phys. Rev. Lett. **102**, 227004 (2009).

[7] W. Bao, Y. Qiu, Q. Huang, M. A. Green, P. Zajdel, M. R. Fitzsimmons, M. Zhernenkov, S. Chang, M. H. Fang, B. Qian, E. K. Vehstedt, J. H. Yang, H. M. Pham, L. Spinu, and Z. Q. Mao, Phys. Rev. Lett. **102**, 247001 (2009).

[8] Q. Huang, Y. Qiu, W.i Bao, M. A. Green, J.W. Lynn, Y. C. Gasparovic, T. Wu, G. Wu, and X. H. Chen, Phys. Rev. Lett. **101**, 257003 (2008).

[9] K. Kaneko, A. Hoser, N. Caroca-Canales, A. Jesche, C. Krellner, O. Stockert, and C. Geibel, Phys. Rev. B **78**, 212502 (2008).

[10] C. Krellner, N. Caroca-Canales, A. Jesche, H. Rosner, A. Ormeci, and C. Geibel, Phys. Rev. B **78**, 100504 (2008).

[11] J. Zhao, D. X. Yao, S. H. Li, T. Hong, Y. Chen, S. Chang, W. Ratcliff II, J.W. Lynn, H. A. Mook, G. F. Chen, J. L. Luo, N. L. Wang, E.W. Carlson, Jiangping Hu, and P. C. Dai, Phys. Rev. Lett. **101**, 167203 (2008).

[12] I. I. Mazin, D. J. Singh, M. D. Johannes, and M. H. Du, Phys. Rev. Lett. **101**, 057003 (2008).

[13] C. Cao, P. J. Hirschfeld, and H. P. Cheng, Phys. Rev. B **77**, 220506(R) (2008).

[14] D. J. Singh and M.-H. Du, Phys. Rev. Lett. **100**, 237003 (2008).

[15] K. Kuroki, S. Onari, R. Arita, H. Usui, Y. Tanaka, H. Kontani, and H. Aoki, Phys. Rev. Lett. **101**, 087004 (2008).

[16] T. Yildirim, Phys. Rev. Lett. **101**, 057010 (2008).

[17] Q. M. Si and E. Abrahams, Phys. Rev. Lett. **101**, 076401 (2008).

[18] F. J. Ma, Z. Y. Lu, and T. Xiang, Phys. Rev. B **78**, 224517 (2008).

[19] C. Fang, H. Yao, W. F. Tsai, J. P. Hu, and S. A. Kivelson, Phys. Rev. B **77**, 224509 (2008).

[20] C. K. Xu, M. M*ü*ller, and S. Sachdev, Phys. Rev. B **78**, 020501(R) (2008).

[21] J. S. Wu, P. Phillips, and A. H. Castro Neto, Phys. Rev. Lett. **101**, 126401 (2008).

[22] Q. Han, Y. Chen and Z. D. Wang, Europhys. Lett. **82**, 37007 (2008).

[23] T. Li, J. Phys.: Condens. Matter **20**, 425203 (2008).

[24] S. Raghu, X. L. Qi, C. X. Liu, D. J. Scalapino, and S. C. Zhang, Phys. Rev. B **77**, 220503 (2008).

[25] I. I. Mazin, M. D. Johannes, L. Boeri, K. Koepernik and D. J. Singh, Phys. Rev. B **78**, 085104 (2008).

[26] K. Haule, J. H. Shim, and G. Kotliar, Phys. Rev. Lett. **104**, 216405 (2008).

[27] K. Kubo, and P. Thalmeier, J. Phys. Soc. Jpn. **78**, 083704 (2009).

[28] R. Yu, K. T. Trinh, A. Moreo, M. Daghofer, J. A. Riera, S. Haas, and E. Dagotto, Phys. Rev. B **79**, 104510 (2009).

[29] P. A. Lee, and X. G. Wen, Phys. Rev. B **78**, 144517 (2008).

[30] M. Daghofer, A. Nicholson, A. Moreo, and E. Dagotto, Phys. Rev. B **81**, 014511 (2010).

[31] S. Zhou, and Z. Q. Wang, Phys. Rev. Lett. **105**, 096401 (2010).

[32] Q. L. Luo, G. Martins, D. X. Yao, M. Daghofer, R. Yu, A. Moreo, and E. Dagotto, Phys. Rev. B **82**, 104508 (2010).

[33] M. Daghofer, Q. L. Luo, R. Yu, D. X. Yao, A. Moreo, and E. Dagotto, Phys. Rev. B **81**, 180514R (2010).

[34] E. Bascones, M.J. Calderón, and B. Valenzuela, Phys. Rev. Lett. **104**, 227201 (2010).

[35] S. Graser, T. A. Maier, P. J. Hirschfeld, and D. J. Scalapino, New Journal of Physics **11**, 025016 (2009).

[36] P. M. R. Brydon, M. Daghofer, and C. Timm, arXiv: 1007.1949 (unpublished).

[37] M. J. Calderón, B. Valenzuela, and E. Bascones, Phys. Rev. B **80**, 094531 (2009).

[38] X. Y. Wang, M. Daghofer, A. Nicholson, A. Moreo, M. Guidry, and E. Dagotto, Phys. Rev. B **81**, 144509 (2010).

[39] S. Graser, A. F. Kemper, T. A. Maier, H. P. Cheng, P. J. Hirschfeld, and D. J. Scalapino, Phys. Rev. B **81**, 214503 (2010).

[40] H. Eschrig, and K. Koepernik, Phys. Rev. B **80**, 104503 (2009).

[41] A. M. Turner, F. Wang, and A. Vishwanath, Phys. Rev. B **80**, 224504 (2009).

[42] W. C. Lv, J. S. Wu, and P. Phillips, Phys. Rev. B **80**, 80-224506 (2009).

[43] C. C. Chen, J. Maciejko, A. P. Sorini, B. Moritz, R. R. P. Singh, and T. P. Devereaux, Phys. Rev. B **82**, 100504R (2010).

[44] T. Shimojima, K. Ishizaka, Y. Ishida, N. Katayama, K. Ohgushi, T. Kiss, M. Okawa, T. Togashi, X. Y.

Wang, C. T. Chen, S. Watanabe, R. Kadota, T. Oguchi, A. Chainani, and S. Shin, Phys. Rev. Lett. **104**, 057002 (2010).

[45] A. Akrap, J. J. Tu, L. J. Li, G. H. Cao, Z. A. Xu, and C. C. Homes, Phys. Rev. B **80**, 180502(R) (2009).

[46] J. Zhao, D. T. Adroja, D. X. Yao, R. Bewley, S. L. Li, X. F. Wang, G.Wu, X. H. Chen, J. P. Hu and P. C. Dai, Nature phys. **5**, 555 (2009).

[47] J. H. Chu, J. G. Analytis, D. Press, K. De Greve, T. D. Ladd, Y. Yamamoto, and I. R. Fisher, Phys. Rev. B **81**, 214502 (2010).

[48] J. H. Chu, J. G. Analytis, K. De Greve, P. L. McMahon, Z. Islam, Y. Yamamoto, I. R. Fisher, Science **329**, 824 (2010).

[49] M. A. Tanatar, E. C. Blomberg, A. Kreyssig, M. G. Kim, N. Ni, A. Thaler, S. L. Bud'ko, P. C. Canfield, A. I. Goldman, I. I. Mazin, R. Prozorov, arXiv: 1002.3801 (unpublished).

[50] A. Dusza, A. Lucarelli, F. Pfuner, J. H. Chu, I. R. Fisher, L. Degiorgi, arXiv: 1007.2543 (unpublished).

[51] C. C. Lee, W. G. Yin, and W. Ku, Phys. Rev. Lett. **103**, 267001 (2009).

[52] F. Krüger, S. Kumar, J. Zaanen, and J. van den Brink, Phys. Rev. B **79**, 054504 (2010).

[53] M. M. Qazilbash, J. J. Hamlin, R. E. Baumbach, L. J. Zhang, D. J. Singh, M. B. Maple, and D. N. Basov, Nature phys. **5**, 647 (2009).

[54] V. Cvetkovic, and Z. Tesanovic, Phys. Rev. B **80**, 024512 (2009).

[55] J. D. Podolsky, H. Y. Kee, and Y. B. Kim, Europhys. Lett. **88**, 17004 (2009).

[56] Z. J. Yao, J. X. Li, Q. Han, Z. D. Wang, arXiv: 1003.1660 (unpublished).

[57] F. Lu, Y. Song, D. M. Chen, and L. J. Zou, Chin. Phys. Lett. **26**, 097501 (2009).

[58] M. Yoshizawa,. R. Kamiya, R. Onodera, and Y. Nakanishi, K. Kihou, H. Eisaki, A. Iyo, and C. H. Lee, arXiv: 1008.1479 (unpublished).

[59] Y. Zhang, F. Chen, C. He, B. Zhou, B. P. Xie, C. Fang, W. F. Tsai, X. H. Chen, H. Hayashi, J. Jiang, H. Iwasawa, K. Shimada, H. Namatame, M. Taniguchi, J. P. Hu, and D. L. Feng, Phys. Rev. B **83**, 054510 (2011).

[60] M. Yi, D. H. Lu, J. H. Chu, J. G. Analytis, A. P. Sorini, A. F. Kemper, S. K. Mo, R. G. Moore, M. Hashimoto, W. S. Lee, Z. Hussain, T. P. Devereaux, I. R. Fisher, and Z. X. Shen, arXiv: 1011.0050 (unpublished).

[61] Y. K. Kim, H. Oh, C. Kim, D. J. Song, W. S. Jung, B. Y. Kim, H. J. Choi, C. Kim, B. S. Lee, S. H. Khim, K. H. Kim, J. B. Hong, and Y. S. Kwon, arXiv: 1011.1112 (unpublished).

[62] G. Li, B. S. Conner, S. Weyeneth, N. D. Zhigadlo, S. Katrych, Z. Bukowski, J. Karpinski, D. J. Singh,

M. D. Johannes, and L. Balicas, arXiv: 1009.1408 (unpublished).